

ReLU Deep Neural Networks and Linear Finite Elements

Juncai He ^{*} Lin Li [†] Jinchao Xu [‡] Chunyue Zheng [§]

Abstract

In this paper, we investigate the relationship between deep neural networks (DNN) with rectified linear unit (ReLU) function as the activation function and continuous piecewise linear (CPWL) functions, especially CPWL functions from the simplicial linear finite element method (FEM). We first consider the special case of FEM. By exploring the DNN representation of its nodal basis functions, we present a ReLU DNN representation of CPWL in FEM. We theoretically establish that at least 2 hidden layers are needed in a ReLU DNN to represent any linear finite element functions in $\Omega \subseteq \mathbb{R}^d$ when $d \geq 2$. Consequently, for $d = 2, 3$ which are often encountered in scientific and engineering computing, the minimal number of two hidden layers are necessary and sufficient for any CPWL function to be represented by a ReLU DNN. Then we include a detailed account on how a general CPWL in \mathbb{R}^d can be represented by a ReLU DNN with at most $\lceil \log_2(d+1) \rceil$ hidden layers and we also give an estimation of the number of neurons in DNN that are needed in such a representation. Furthermore, using the relationship between DNN

^{*}School of Mathematical Sciences, Peking University, Beijing 100871, China. Email: juncaihe@pku.edu.cn

[†]Beijing International Center for Mathematical Research, Peking University, Beijing 100871, China. Email: lilin1993@pku.edu.cn

[‡]Department of Mathematics, Pennsylvania State University, State College, PA 16802, USA. Email: xu@math.psu.edu

[§]Department of Mathematics, Pennsylvania State University, State College, PA 16802, USA. Email: cmz5199@psu.edu

and FEM, we theoretically argue that a special class of DNN models with low bit-width are still expected to have an adequate representation power in applications. Finally, as a proof of concept, we present some numerical results for using ReLU DNNs to solve a two point boundary problem to demonstrate the potential of applying DNN for numerical solution of partial differential equations.

1 Introduction

In recent years, deep learning models have achieved unprecedented success in various tasks of machine learning or artificial intelligence, such as computer vision, natural language processing and reinforcement learning [1]. One main technique in deep learning is deep neural network. A typical DNN model is based on a hierarchy of composition of linear functions and a given nonlinear activation function. However, why DNN models can work so well is still unclear.

Mathematical analysis of DNN can be carried out using many different approaches. One approach is to study the approximation properties of the function class provided by DNN. The approximation property of DNN is relevant to the so-called expressive power [2] of a DNN model. Early studies of approximation properties of DNN can be traced back in [3] and [4] where the authors established some approximation properties for the function classes given by a feedforward neural network with a single hidden layer. Further error estimates for such neural networks in terms of number of neurons can be found in [5] for sinusoidal activation functions and in [6] for more general sigmoidal activation functions. There are many other papers on this topic during the 90s and a good review of relevant works can be found in [7] and [8].

There are many different choices of activation functions. In fact, as shown in [9], a neural network with a single hidden layer can approximate any continuous function for any activation function which is not a polynomial. Among all the activation functions, the so-called rectified linear unit (ReLU) activation function [10], namely $\text{ReLU}(x) = \max(x, 0)$, has emerged to be one of the most popular activation functions

used in the deep learning literature and applications. [11] presents an approximation of ReLU DNNs by relating to wavelets. Recently, [12] establish L^∞ and L^2 error bounds for functions of many variables that are approximated by linear combinations of ReLU. [13] presents rates of approximation by deep CNNs for functions in the Sobolev space $H^r(\Omega)$ with $r > 2 + d/2$. This paper is devoted to some further mathematical analysis of DNN models with ReLU as the activation function.

It is not difficult to see that the following statement is true: “*Every ReLU DNN function in \mathbb{R}^d represents a continuous piecewise linear (CPWL) function defined on a number of polyhedral subdomains.*” One important recent development is that the converse of the above statement has also been proven true. More specifically, the following result is established by [14] based on an earlier result by [15] on lattice representation of DNN: “*Every CPWL function in \mathbb{R}^d can be represented by a ReLU DNN model with at most $\lceil \log_2(d + 1) \rceil$ hidden layers.*”

Motivated by this result, we study the following two questions on the DNN representation of a given CWPL function:

1. How many numbers of neurons are needed?
2. What is the minimal number of layers that are needed?

To answer the first question, in this paper, we will go through the proof of this representation result to give some explicit estimations of the number of neurons that are needed in a DNN to represent a given CPWL function. As a result, we find that the number of neurons that are needed for a DNN to represent a CPWL on m -subdomains can be as large as $\mathcal{O}(d2^{mm!})!$

In order to obtain DNN representation with fewer numbers of neurons, in this paper, we consider a special class of CPWL functions, namely the linear finite element (LFE) functions [16] defined on a collection of special subdomains, namely simplexes in \mathbb{R}^d . As every finite element function can be written as a linear combination of nodal basis functions, it suffices to study DNN representation of any given nodal basis function. To represent a nodal basis function by a DNN, we do not need to consider the complicated domain partition related with lattice representation([15]),

which is important in representing general piecewise linear functions in \mathbb{R}^d ([14]). We prove that a linear finite element function with N degrees of freedom can be represented by a ReLU DNN with at most $\mathcal{O}(d\kappa^d N)$ number of neurons with $\mathcal{O}(d)$ hidden layers where $\kappa \geq 2$) depends on the shape regularity of the underlying finite element grid.

To answer the second question, we will again consider the linear finite element functions. In this paper, we will show (see Theorem 4.1) that at least 2 hidden layers are needed for a ReLU DNN to represent any linear finite element function in a bounded domain $\Omega \subset \mathbb{R}^d$ or \mathbb{R}^d when $d \geq 2$. The $\lceil \log_2(d+1) \rceil$ number of hidden layers is also optimal for $d = 2, 3$. Whether this number is also optimal for $d > 3$ is still an open problem.

In real applications, many efforts have been made to compress the deep neural networks by using heavily quantized weights, c.f. [17]. Especially, binary and ternary weight models not only give high model compression rate, but also eliminate the need of most floating-point multiplications during inference phase. In particular, for some small data sets such as MINST [18] and CIFAR-10 [19], the ternary CNNs [20] are shown to have the same accuracy as that of the original CNN. Using the special structure for representing any CPWL functions by ReLU DNNs, we provide certain theoretical justification of the use of ternary CNNs. Furthermore, we also present a modified version of those models with some rigorous mathematical justifications.

Another topic that will be investigated in the paper is the application of artificial neural networks for differential equations. This topic can be traced back to [22, 23, 21] in which collocation methods are studied. Recently, there are increased new research interests in the literature for the application of deep neural networks for numerical approximation of nonlinear and high dimensional PDEs as in [25, 24, 26]. Based on our result about the relationship between FEM and ReLU DNNs, we discuss the application of ReLU DNN for solving PDEs with respect to the convergence properties. In particular, we use an 1D example to demonstrate that a Galerkin method using ReLU DNN can lead to better approximation result than adaptive finite element method that has exactly the same number of degrees of freedom as in the ReLU DNN.

The remaining sections are organized as follows. In §2, we introduce some notation and preliminary results about ReLU DNNs. In §3 we investigate the relationship between FEM and ReLU DNN. In §4 we prove that at least 2 hidden layers are needed to represent any LFE functions by ReLU DNN in $\Omega \subset \mathbb{R}^d$ for $d \geq 2$. In §5, we give the self contained proof of representing CPWL and LFE functions with $\lceil \log_2(d+1) \rceil$ hidden layers and give the size estimation. In §6 we show that a special structure of ReLU DNN can also recover any CPWL function. In §7 we investigate the application of DNN for numerical PDEs. In §8 we give concluding remarks.

2 Deep neural network (DNN) generated by ReLU

In this section, we briefly discuss the definition and properties of the deep neural networks generated by using ReLU as the activation function.

2.1 General DNN

Given $n, m \geq 1$, the first ingredient in defining a deep neural network (DNN) is (vector) linear functions of the form

$$\Theta : \mathbb{R}^n \rightarrow \mathbb{R}^m, \tag{2.1}$$

as $\Theta(x) = Wx + b$ where $W = (w_{ij}) \in \mathbb{R}^{m \times n}$, $b \in \mathbb{R}^m$.

The second main ingredient is a nonlinear activation function, usually denoted as

$$\sigma : \mathbb{R} \rightarrow \mathbb{R}. \tag{2.2}$$

By applying the function to each component, we can extend this naturally to

$$\sigma : \mathbb{R}^n \mapsto \mathbb{R}^n.$$

Given $d, c, k \in \mathbb{N}^+$ and

$$n_1, \dots, n_k \in \mathbb{N} \text{ with } n_0 = d, n_{k+1} = c,$$

a general DNN from \mathbb{R}^d to \mathbb{R}^c is given by

$$\begin{aligned} f(x) &= f^k(x), \\ f^\ell(x) &= [\Theta^\ell \circ \sigma](f^{\ell-1}(x)) \quad \ell = 1 : k, \end{aligned}$$

with $f^0(x) = \Theta(x)$. The following more concise notation is often used in computer science literature:

$$f(x) = \Theta^k \circ \sigma \circ \Theta^{k-1} \circ \sigma \cdots \circ \Theta^1 \circ \sigma \circ \Theta^0(x), \quad (2.3)$$

here $\Theta^i : \mathbb{R}^{n_i} \rightarrow \mathbb{R}^{n_{i+1}}$ are linear functions as defined in (2.1). Such a DNN is called a $(k+1)$ -layer DNN, and is said to have k hidden layers. Unless otherwise stated, all layers mean hidden layers in the rest of this paper. The size of this DNN is $n_1 + \cdots + n_k$. In this paper, we mainly consider a special activation function, known as the *rectified linear unit* (ReLU), and defined as $\text{ReLU} : \mathbb{R} \mapsto \mathbb{R}$,

$$\text{ReLU}(x) = \max(0, x), \quad x \in \mathbb{R}. \quad (2.4)$$

A ReLU DNN with k hidden layers might be written as:

$$f(x) = \Theta^k \circ \text{ReLU} \circ \Theta^{k-1} \circ \text{ReLU} \cdots \circ \Theta^1 \circ \text{ReLU} \circ \Theta^0(x). \quad (2.5)$$

We note that ReLU is a continuous piecewise linear (CPWL) function. Since the composition of two CPWL functions is obviously still a CPWL function, we have the following simple observation([14]).

Lemma 2.1 *Every ReLU DNN: $\mathbb{R}^d \rightarrow \mathbb{R}^c$ is a continuous piecewise linear function. More specifically, given any ReLU DNN, there is a polyhedral decomposition of \mathbb{R}^d such that this ReLU DNN is linear on each polyhedron in such a decomposition.*

Here is a simple example for the “grid” created by some 2-layer ReLU DNNs in \mathbb{R}^2 .

In the rest of the paper, we will use the terminology of CPWL to define the class of functions that are globally continuous and locally linear on each polyhedron in a given finite polyhedral decomposition of \mathbb{R}^d .

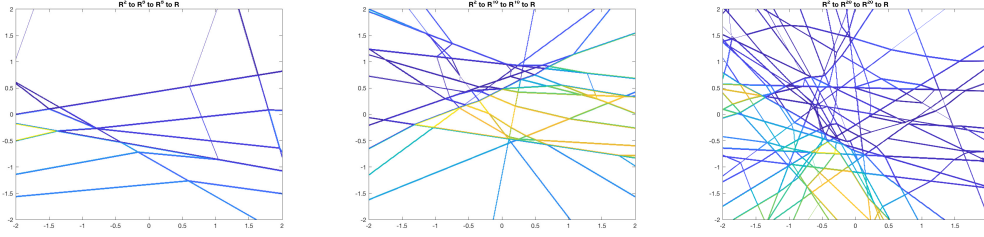


Figure 2.1: Projections of the domain partitions formed by 2-layer ReLU DNNs with sizes $(n_0, n_1, n_2, n_3) = (2, 5, 5, 1), (2, 10, 10, 1)$ and $(2, 20, 20, 1)$ with random parameters.

For convenience of exposition, we introduce the following notation:

$$\begin{aligned} \text{DNN}_J := \{f : f = \Theta^J \circ \text{ReLU} \circ \Theta^{J-1} \dots \text{ReLU} \circ \Theta^0(x), \\ \Theta^\ell \in \mathbb{R}^{n^{\ell+1} \times (n^\ell+1)}, \quad n^0 = d, \quad n^{J+1} = 1, \quad n^\ell \in \mathbb{N}^+\}. \end{aligned} \quad (2.6)$$

Namely DNN_J represents the DNN model with J hidden layers and ReLU activation function with arbitrary size.

2.2 A shallow neural network DNN_1

We note that for $J = 0$, DNN_0 is a simple function space of global linear functions, which is often used in classic statistical analysis such as linear regression. The structure of DNN_J gets more interesting as J becomes larger. We shall now discuss the simple case when $J = 1$, namely

$$\text{DNN}_1^m = \left\{ f : f = \sum_{i=1}^m \alpha_i \text{ReLU}(w_i x + b_i) + \beta \right\}, \quad (2.7)$$

where $\alpha_i, b_i, \beta \in \mathbb{R}, w_i \in \mathbb{R}^{1 \times d}$, for $i = 1, 2, \dots, m$. Here we introduce the superscript m to denote the number of neurons. This simple neural network already has rich mathematical structures and approximation properties. Given a bounded domain $\Omega \subset \mathbb{R}^d$, we introduce the following notation

$$\text{DNN}_1^m(\Omega) = \{f : f(x) \in \text{DNN}_1^m, \quad x \in \Omega \subset \mathbb{R}^d\}, \quad (2.8)$$

as the restriction of DNN_1^m on Ω .

Approximation property for the function class $\text{DNN}_1^m(\Omega)$ has been much studied in the literature. For example, in [3] and [4], $\text{DNN}_1^m(\Omega)$ is proved to be dense in $C^0(\Omega)$ as $m \rightarrow \infty$, which is known as universal approximation. There are also many works devoted to the asymptotic error estimates. For example, [6] established the following estimate:

$$\inf_{g \in \text{DNN}_1^m(\Omega)} \|f - g\|_{0,2,\Omega} \lesssim |\Omega|^{1/2} m^{-\frac{1}{2}} \int_{\mathbb{R}^d} |\omega|_{\Omega} |\hat{f}(\omega)| d\omega, \quad (2.9)$$

where $|\Omega|$ denotes the volume of Ω and

$$|\omega|_{\Omega} = \sup_{x \in \Omega} |\omega \cdot (x - x_{\Omega})|,$$

for some point $x_{\Omega} \in \Omega$.

For a given set of w^i and b^i , it is tempting to think the functions in DNN_1^m are generated by $\{\text{ReLU}(w_i x + b_i)\}_{i=1}^m$. In such a consideration, the following result is of great theoretical interest. The proof will be seen in Section 4.

Theorem 2.1 *$\{\text{ReLU}(w_i x + b_i)\}_{i=1}^m$ are linearly independent if (w_i, b_i) and (w_j, b_j) are linearly independent in $\mathbb{R}^{1 \times (d+1)}$ for any $i \neq j$.*

In real applications, w_i and b_i are variables. As a result, DNN_1^m is generated by variable basis functions $\{\text{ReLU}(w_i x + b_i)\}_{i=1}^m$ and in particular DNN_1^m is a non-linear space which is expected to have certain nonlinear approximation property as discussed in [27].

3 Linear finite element (LFE) function as a DNN

In this section, we consider a special CPWL function space, namely the space of linear simplicial finite element functions. We will first give a brief description of finite element method and give a constructive proof that any linear simplicial finite element function can be represented by a ReLU DNN.

3.1 Linear finite element spaces

The finite element method (FEM), as a popular numerical method for approximating the solutions of partial differential equations (PDEs), is a well-studied subject ([16],[28]). The finite element function space is usually a subspace of the solution space, for example, the space of piecewise linear functions over a given mesh. In [14], it is shown that piecewise linear functions can be written as ReLU DNNs, which will be discussed in details later. By exploring the relationship between FEM and ReLU DNN, we hope to shed some new light on how DNN works in this special case.

Assuming that $\Omega \subset \mathbb{R}^d$ is a bounded domain. We consider a special finite element function class consisting of CPWL functions with respect to a simplicial partition of Ω . Such simplicial partitions are often known as finite element grids or meshes. Some typical finite element grids are shown in Figure 3.1 for $d = 1, 2, 3$.

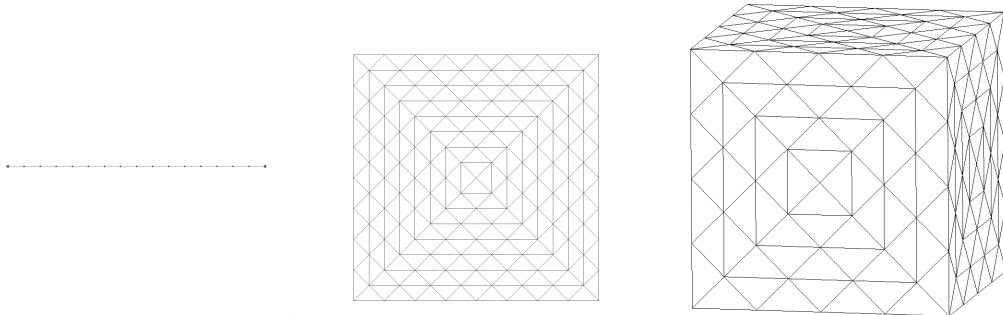


Figure 3.1: an interval, a triangle and a tetrahedron partition

A finite element space is defined in association with a simplicial finite element grid $\mathcal{T}_h \subset \Omega$. A simplicial finite element grid \mathcal{T}_h consists of a set of simplexes $\{\tau_k\}$ and the corresponding set of nodal points is denoted by \mathcal{N}_h . For a given grid \mathcal{T}_h , the corresponding finite element space is given by

$$V_h = \{v \in C(\Omega) : v \text{ is linear on each element } \tau_k \in \mathcal{T}_h\}. \quad (3.1)$$

Given $x_i \in \mathcal{N}_h$, it is easy to see that there exists a unique function $\phi_i \in V_h$, known

as the nodal basis function, such that

$$\phi_i(x_j) = \delta_{ij}, \quad x_j \in \mathcal{N}_h. \quad (3.2)$$

A typical profile of ϕ_i is shown in Fig. 3.2 for $d = 1$ and $d = 2$.

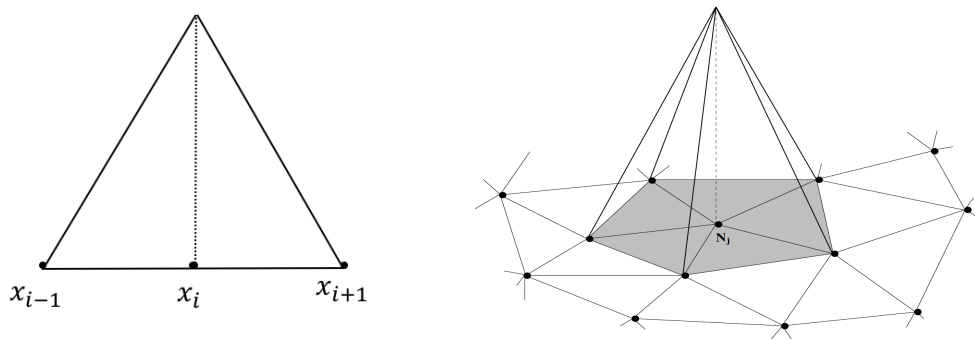


Figure 3.2: The basis function in 1D and 2D

Obviously any $v \in V_h$ can be uniquely represented in terms of these nodal basis functions:

$$v(x) = \sum_{i=1}^N \nu_i \phi_i(x), \quad (3.3)$$

where N is the degrees of freedom.

Given $x_i \in \mathcal{N}_h$, let $N(i)$ denote all the indices j such that τ_j contains the nodal point x_i , namely

$$N(i) = \{j : x_i \in \tau_j\},$$

and k_h denote the maximum number of neighboring elements in the grid

$$k_h \equiv d(\mathcal{T}_h) = \max_{x_i \in \mathcal{N}_h} |N(i)|. \quad (3.4)$$

Let $G(i)$ denote the support of the nodal basis ϕ_i :

$$G(i) = \bigcup_{k \in N(i)} \tau_k.$$

We say that the grid \mathcal{T}_h is locally convex if $G(i)$ is convex for each i .

We proceed next to demonstrate how a finite element function can be represented by a ReLU DNN. Our derivation and analysis are based on the representation of the finite element function as a linear combination of basis functions as follows.

3.2 DNN representation of finite element functions

As an illustration, we will now demonstrate how a linear finite element function associated with a locally convex grid \mathcal{T}_h can be represented by a ReLU DNN. For more general grids, we refer to Remark 1 and §5.

Thanks to (3.3), it suffices to show that each basis function ϕ_i can be represented by a ReLU DNN. We first note that the case where $d = 1$ is trivial as the basis function ϕ_i with support in $[x_{i-1}, x_{i+1}]$ can be easily written as

$$\phi_i(x) = \frac{1}{h_{i-1}} \text{ReLU}(x - x_{i-1}) - \left(\frac{1}{h_{i-1}} + \frac{1}{h_i}\right) \text{ReLU}(x - x_i) + \frac{1}{h_i} \text{ReLU}(x - x_{i+1}), \quad (3.5)$$

where $h_i = x_{i+1} - x_i$.

In order to consider the cases where $d > 1$, we first prove the following lemma.

Lemma 3.1 *Given $x_i \in \mathcal{N}_h$, if $G(i)$ is convex, then the corresponding basis function can be written as*

$$\phi_i(x) = \max \left\{ 0, \min_{k \in N(i)} g_k(x) \right\}, \quad (3.6)$$

where, for each $k \in N(i)$, g_k is the global linear function such that $g_k = \phi_i$ on τ_k .

Proof To show (3.6) holds for all $x \in \mathbb{R}^d$, we first consider the case $x \in G(i)$, namely $x \in \tau_{k_0}$ for some $k_0 \in N(i)$. Thus

$$\phi_i(x) = g_{k_0}(x) \geq 0. \quad (3.7)$$

Let P_k be the hyperplane that passes through the $d - 1$ subsimplex (of τ_k) that does not contain x_i (see the left figure in Figure 3.3). Since $G(i)$ is convex by assumption,

all points in τ_{k_0} should be on the same side of the hyperplane P_k . As a result, for all $k \in N(i)$,

$$g_k(y) \geq 0 \equiv g_{k_0}(y), \quad y \in P_{k_0} \cap \tau_{k_0}.$$

By combining the above inequality with the following obvious inequality that

$$g_k(x_i) = 1 \geq 1 = g_{k_0}(x_i), \quad k \in N(i),$$

and the fact that all g_k are linear, we conclude that

$$g_k(y) \geq g_{k_0}(y), \quad \forall y \in \tau_{k_0}, k \in N(i).$$

In particular

$$g_k(x) \geq g_{k_0}(x), \quad k \in N(i).$$

This, together with (3.7), proves that (3.6) holds for all $x \in G(i)$. Thus

$$\max \left\{ 0, \min_{k \in N(i)} g_k(x) \right\} = g_{k_0}(x). \quad (3.8)$$

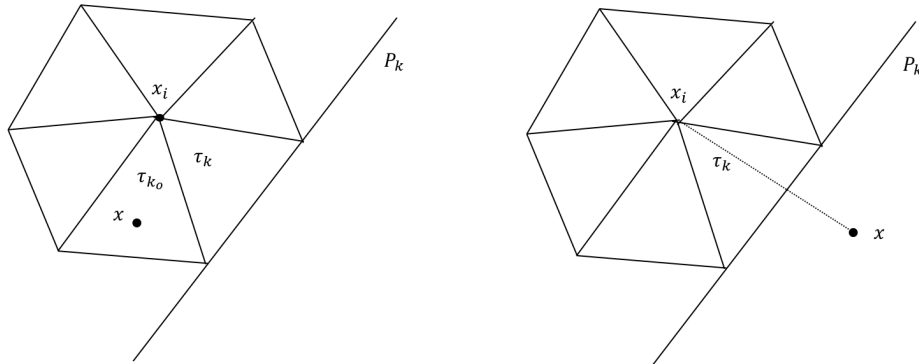


Figure 3.3: Left: $x \in G(i)$, right: $x \notin G(i)$

On the other hand, if $x \notin G(i)$, there exists a $\tau_k \subset G(i)$ such that τ_k contains a segment of the straight line that pass through x and x_i (see the right figure in Figure

3.3). Again let P_k be the hyperplane associated with τ_k as defined above. We note that x and x_i are on the different sides of P_k . Since

$$g_k(x_i) \geq 0, \quad g_k(y) = 0, \quad y \in P_k,$$

we then have

$$\min_{k \in N(i)} g_k(x) \leq g_k(x) \leq 0,$$

which implies

$$\max \left\{ 0, \min_{k \in N(i)} g_k(x) \right\} = 0 = \phi_i(x), \quad x \notin G(i).$$

This finishes the proof of Lemma 3.1. □

Remark 1 *If $G(i)$ is not convex, we could also write the basis function as some max-min functions. But the form of max-min function is not as simple as the case where $G(i)$ is convex, and it depends on the shape of the support of the basis function. In some cases, we can write the basis function as the max-min-max form if $G(i)$ is a special non-convex set.*

We are now in a position to state and prove the main result in this section.

Theorem 3.1 *Given a locally convex finite element grid \mathcal{T}_h , any linear finite element function with N degrees of freedom, can be written as a ReLU-DNN with at most $k = \lceil \log_2 k_h \rceil + 1$ hidden layers and at most $\mathcal{O}(k_h N)$ number of the neurons.*

Proof We have the following identity,

$$\min\{a, b\} = \frac{a+b}{2} - \frac{|a-b|}{2} = v \cdot \text{ReLU}(W \cdot [a, b]^T), \quad (3.9)$$

where

$$v = \frac{1}{2}[1, -1, -1, -1], \quad W = \begin{bmatrix} 1 & 1 \\ -1 & -1 \\ 1 & -1 \\ -1 & 1 \end{bmatrix}.$$

By Lemma 3.1, the basis function $\phi_i(x)$ can be written as:

$$\phi_i(x) = \max \left\{ 0, \min_{k \in N(i)} g_k(x) \right\}.$$

For convenience, we assume that

$$N(i) = \{r_1, r_2, \dots, r_{|N(i)|}\}.$$

Then we have

$$\begin{aligned} \min_{k \in N(i)} g_k(x) &= \min \{g_{r_1}(x), \dots, g_{r_{|N(i)|}}(x)\} \\ &= \min \left\{ \min\{g_{r_1}, \dots, g_{r_{\lceil |N(i)|/2}}\}, \min\{g_{r_{\lceil |N(i)|/2}+1}, \dots, g_{r_{|N(i)|}}\} \right\} \\ &= v \cdot \text{ReLU} \left(W \cdot \begin{bmatrix} \min\{g_{r_1}, \dots, g_{r_{\lceil |N(i)|/2}}\} \\ \min\{g_{r_{\lceil |N(i)|/2}+1}, \dots, g_{r_{|N(i)|}}\} \end{bmatrix} \right). \end{aligned}$$

According to this procedure, we get the minimum of $|N(i)|$ terms by splitting them in two, each taking the minimum over at most $\lceil |N(i)|/2 \rceil$ terms. This contributes to one ReLU hidden layer. Then we can further split the terms

$$\min\{g_{r_1}, \dots, g_{r_{\lceil |N(i)|/2}}\}, \quad \min\{g_{r_{\lceil |N(i)|/2}+1}, \dots, g_{r_{|N(i)|}}\}$$

until all the minimum functions contain only 1 or 2 terms.

1. If there is one term

$$\min\{a\} = a.$$

2. If there are two terms

$$\min\{a, b\} = v \cdot \text{ReLU}(W \cdot [a, b]^T).$$

which is also a ReLU DNN with 1 hidden layer. So we can write a basis function as a $1 + \lceil \log_2 k_h \rceil$ -hidden-layer DNN. Considering the binary-tree structure, a k -layer full binary-tree has $2^k - 1$ nodes. We can see the number of neurons is at most

$$\mathcal{O}(2^k) = \mathcal{O}(2^{1+\lceil \log_2 k_h \rceil}) = \mathcal{O}(k_h).$$

By (3.3), the piecewise linear function can be represented as a DNN with $k = 1 + \lceil \log_2 k_h \rceil$ hidden layers. The number of neurons is at most $\mathcal{O}(k_h N)$. \square

We now consider a special class of the so-called shape regular finite element grid \mathcal{T}_h which satisfies

$$\kappa_1 \leq \frac{r_\tau}{R_\tau} \leq \kappa_2, \quad \forall \tau \in \mathcal{T}_h, \quad (3.10)$$

for some constants κ_1 and κ_2 independent of h and d , where r_τ (R_τ) is the radius of the largest (smallest) ball contained in (containing) τ .

Corollary 3.1 *Given a locally convex and shape regular finite element grid \mathcal{T}_h , any linear finite element function with N degrees of freedom (DOFs), can be written as a ReLU-DNN with at most $\mathcal{O}(d)$ hidden layers. The number of neurons is at most $\mathcal{O}(\kappa^d N)$ for some constant $\kappa \geq 2$ depending on the shape-regularity of \mathcal{T}_h . The number of non-zero parameters is at most $\mathcal{O}(d\kappa^d N)$.*

We note that, using the approach described in this section, a finite element function with N DOFs can be represented by a DNN with $\mathcal{O}(N)$ number of weights. This property is expected to be useful when DNNs are used in adaptive mesh-less or vertex-less numerical discretization methods for partial differential equation, which is a subject of further study.

3.3 Comparison of error estimates in adaptive finite element and DNN methods

Error estimates for adaptive finite element methods are well studied in the literature. For example, an appropriately adapted linear finite element function with $\mathcal{O}(N)$ DOFs is proved to admit the following error estimate:

$$\inf_{v \in V_h} \|u - v\|_{0,2,\Omega} \leq CN^{-\frac{2}{d}} |u|_{2, \frac{2d}{d+2}, \Omega}, \quad (3.11)$$

if $u \in W^{2, \frac{2d}{d+2}}(\Omega)$ and v is the interpolation based on the adapted finite element grid. More details can be founded in [29, 27].

For a shallow network DNN_1 with $\mathcal{O}(N)$ DOFs (i.e. $\mathcal{O}(\frac{N}{d})$ neurons), we have the next error estimate in (2.9) as

$$\min_{v \in \text{DNN}_{\frac{N}{d}}(\Omega)} \|u - v\|_{0,2,\Omega} \lesssim |\Omega|^{1/2} \left(\frac{N}{d}\right)^{-\frac{1}{2}} \int_{\mathbb{R}^d} |\omega|_{\Omega} |\hat{u}(\omega)| d\omega. \quad (3.12)$$

In comparison, an adaptive finite element function with the same order of $\mathcal{O}(N)$ DOFs can only have convergence rate of order $\mathcal{O}(N^{-\frac{2}{d}})$.

As will be shown in §4, shallow neural networks DNN_1 (namely with only one hidden layer) cannot recover a linear finite element function in general, but may potentially lead to better asymptotic accuracy as the dimension d gets larger.

One idea that may help us to understand is that the shallow network is a kind of N -term or basis selection ([27]) approximation scheme with $\{\sigma(w_i x + b_i)\}_{i=1}^N$ as the basis functions (as shown in Theorem 2.1), similar to using $\{\sin(nx)\}_{n=1}^N$ as the basis functions in Fourier approximation or some others in wavelets.

For deep ReLU neural networks, our connections of FEM and ReLU DNNs in this section help us to construct a special ReLU DNN models with depth $\mathcal{O}(d)$ and parameters $\mathcal{O}(dk_d N)$ for $\mathcal{O}(N)$ DOFs. By using the approximation result for adaptive FEM, DNN approximation u_{DNN} for special structure with $\mathcal{O}(N)$ DOFs can get

$$\|u - u_{\text{DNN}}\|_{0,2,\Omega} \lesssim \left(\frac{N}{dk_d}\right)^{-\frac{2}{d}} |u|_{1, \frac{2d}{2+d}, \Omega} \lesssim (N)^{-\frac{2}{d}} |u|_{1, \frac{2d}{2+d}, \Omega}, \quad (3.13)$$

and $k_d = \mathcal{O}(\kappa^d)$. This shows that there exists some special deep ReLU DNN structure which is at least as good as adaptive FEM.

4 LFE can not be recovered by DNN_1 for $d \geq 2$

In the previous section, we show that a finite element function can be represented by a ReLU DNN with $\log_2 k_h + 1$ hidden layers.

In view of Lemma 2.1 and the fact that $\text{DNN}_J \subseteq \text{DNN}_{J+1}$, it is natural to ask that how many layers are needed at least to recover all linear finite element functions in \mathbb{R}^d . In this section, we will show that

$$J_d \geq 2, \quad \text{if } d \geq 2, \quad (4.1)$$

where J_d is the minimal J such that all linear finite element functions in \mathbb{R}^d can be recovered by DNN_J .

In particular, we will show the following theorem.

Theorem 4.1 *If $\Omega \subset \mathbb{R}^d$ is either a bounded domain or $\Omega = \mathbb{R}^d$, DNN_1 can not be used to recover all linear finite element functions in Ω .*

Proof We prove it by contradiction. Let us assume that for any continuous piecewise linear function $f : \Omega \rightarrow \mathbb{R}$, we can find finite $N \in \mathbb{N}$, $w_i \in \mathbb{R}^{1,d}$ as row vector and $\alpha_i, b_i, \beta \in \mathbb{R}$ such that

$$f = \sum_{i=1}^N \alpha_i \text{ReLU}(w_i x + b_i) + \beta,$$

with $f_i = \alpha_i \text{ReLU}(w_i x + b_i)$, $\alpha_i \neq 0$ and $w_i \neq 0$. Consider the finite element functions, if this one hidden layer ReLU DNN can recover any basis function of FEM, then it can recover the finite element space. Thus let us assume f is a locally supported basis function for FEM, i.e. $\text{supp}(f)$ is bounded, where

$$\text{supp}(f) := \overline{\{x \in \Omega \mid f(x) \neq 0\}}.$$

Furthermore, if Ω is a bounded domain, we assume that

$$d(\text{supp}(f), \partial\Omega) > 0, \quad (4.2)$$

with

$$d(A, B) = \inf_{x \in A, y \in B} \|x - y\|,$$

as the distance of two closed sets.

A more important observation is that $\nabla f : \Omega \rightarrow \mathbb{R}^d$ is a piecewise constant vector function. The key point is to consider the discontinuous points for $g := \nabla f = \sum_{i=1}^N \nabla f_i$.

For more general case, we can define the set of discontinuous points of a function by

$$D_g := \{x \in \Omega \mid x \text{ is a discontinuous point of } g\}.$$

Because of the property that

$$D_{f+g} \supseteq D_f \cup D_g \setminus (D_f \cap D_g), \quad (4.3)$$

we have

$$D_{\sum_{i=1}^N g_i} \supseteq \bigcup_{i=1}^N D_{g_i} \setminus \bigcup_{i \neq j} (D_{g_i} \cap D_{g_j}). \quad (4.4)$$

Note that

$$g_i = \nabla f_i(x) = \nabla (\alpha_i \text{ReLU}(w_i x + b_i)) = (\alpha_i H(w_i x + b_i)) w_i \in \mathbb{R}^d, \quad (4.5)$$

for $i = 1 : N$ with H be the Heaviside function defined as:

$$H(x) = \begin{cases} 0 & \text{if } x \leq 0, \\ 1 & \text{if } x > 0. \end{cases}$$

This means that

$$D_{g_i} = \{x \mid w_i x + b_i = 0\} \quad (4.6)$$

is a $d - 1$ dimensional affine space in \mathbb{R}^d .

Without loss of generality, we can assume that

$$D_{g_i} \neq D_{g_j}. \quad (4.7)$$

When the other case occurs, i.e. $D_{g_{\ell_1}} = D_{g_{\ell_2}} = \dots = D_{g_{\ell_k}}$, by the definition of g_i in (4.5) and D_{g_i} in (4.6), this happens if and only if there is a row vector (w, b) such that

$$c_{\ell_i} (w \quad b) = (w_{\ell_i} \quad b_{\ell_i}), \quad (4.8)$$

with some $c_{\ell_i} \neq 0$ for $i = 1 : k$. We combine those g_{ℓ_i} as

$$\tilde{g}_\ell = \sum_{i=1}^k g_{\ell_i} = \sum_{i=1}^k \alpha_{\ell_i} H(w_{\ell_i} x + b_{\ell_i}) w_{\ell_i}, \quad (4.9)$$

$$= \sum_{i=1}^k (c_{\ell_i} \alpha_{\ell_i} H(c_{\ell_i}(wx + b))) w, \quad (4.10)$$

$$= \begin{cases} \left(\sum_{i=1}^k c_{\ell_i} \alpha_{\ell_i} H(c_{\ell_i}) \right) w & \text{if } wx + b > 0, \\ \left(\sum_{i=1}^k c_{\ell_i} \alpha_{\ell_i} H(-c_{\ell_i}) \right) w & \text{if } wx + b \leq 0. \end{cases} \quad (4.11)$$

Thus, if

$$\left(\sum_{i=1}^k c_{\ell_i} \alpha_{\ell_i} H(c_{\ell_i}) \right) = \left(\sum_{i=1}^k c_{\ell_i} \alpha_{\ell_i} H(-c_{\ell_i}) \right),$$

\tilde{g}_ℓ is a constant vector function, that is to say $D_{\sum_{i=1}^k g_{\ell_i}} = D_{\tilde{g}_\ell} = \emptyset$. Otherwise, \tilde{g}_ℓ is a piecewise constant vector function with the property that

$$D_{\sum_{i=1}^k g_{\ell_i}} = D_{\tilde{g}_\ell} = D_{g_{\ell_i}} = \{x \mid wx + b = 0\}.$$

This means that we can use condition (4.8) as an equivalence relation and split $\{g_i\}_{i=1}^N$ into some groups, and we can combine those g_{ℓ_i} in each group as what we do above. After that, we have

$$\sum_{i=1}^N g_i = \sum_{\ell=1}^{\tilde{N}} \tilde{g}_\ell,$$

with $D_{\tilde{g}_s} \neq D_{\tilde{g}_t}$. Finally, we can have that $D_{\tilde{g}_s} \cap D_{\tilde{g}_t}$ is an empty set or a $d - 2$ dimensional affine space in \mathbb{R}^d . Since $\tilde{N} \leq N$ is a finite number,

$$D := \bigcup_{i=1}^N D_{\tilde{g}_\ell} \setminus \bigcup_{s \neq t} (D_{\tilde{g}_s} \cap D_{\tilde{g}_t})$$

is an unbounded set.

- If $\Omega = \mathbb{R}^d$,

$$\text{supp}(f) \supseteq D_g = D_{\sum_{i=1}^N g_i} = D_{\sum_{\ell=1}^{\tilde{N}} \tilde{g}_\ell} \supseteq D,$$

is contradictory to the assumption that f is locally supported.

- If Ω is a bounded domain,

$$d(D, \partial\Omega) = \begin{cases} s > 0 & \text{if } D_{\tilde{g}_i} \cap \Omega = \emptyset, \forall i \\ 0 & \text{otherwise.} \end{cases}$$

Note again that all $D_{\tilde{g}_i}$'s are $d - 1$ dimensional affine spaces, while $D_{\tilde{g}_i} \cap D_{\tilde{g}_j}$ is either an empty set or a $d-2$ dimensional affine space. If $d(D, \partial\Omega) > 0$, this implies that ∇f is continuous in Ω , which contradicts the assumption that f is a basis function in FEM. If $d(D, \partial\Omega) = 0$, this contradicts the previous assumption in (4.2).

Hence DNN_1 cannot recover any piecewise linear function in Ω for $d \geq 2$. \square

Following the proof above, we can prove Theorem 2.1.

Proof If (w_i, b_i) and (w_j, b_j) are linearly independent for any $i \neq j$, we know that the set of discontinuous points for any nontrivial combinations of $\nabla_x \text{ReLU}(w_i x + b_i)$ cannot be empty. So, this is contradictory to

$$f = \sum_{i=1}^m \alpha_i \text{ReLU}(w_i x + b_i) = 0,$$

since $D_{\nabla f} \neq \emptyset$ where $f(x)$ is a combination of $\{\text{ReLU}(w_i x + b_i)\}$. \square

This shows that despite it has the so-called universal approximation properties [3, 4], shallow network is not enough in the case of recovering all CPWL functions. More precisely, although the shallow ReLU DNNs are CPWL functions themselves and can approximate any CPWL functions with any accuracy, there are some CPWL functions they cannot represent exactly. As an example, a local basis function in FEM with compact support and some other simple conditions cannot be represented by ReLU DNNs with one hidden layer for dimensions greater than 2.

As for the upper bound, Theorem 5.2 in [14] provides us with one answer.

Corollary 4.1

$$2 \leq J_d \leq \lceil \log_2(d+1) \rceil. \quad (4.12)$$

This also indicates that $\lceil \log_2(d+1) \rceil$ is “optimal” for $d = 2, 3$.

5 General CPWL as a ReLU DNN

In the previous sections, we present a special approach to represent a linear simplicial finite element function by a ReLU DNN. In this section, we discuss a general approach to represent a general CPWL by a ReLU DNN, which is introduced in [14]. In comparison with the special approach in §3, this general approach gives a ReLU DNN with relatively fewer layers but significantly more number of neurons.

5.1 The main result

Assume that $f : \mathbb{R}^d \rightarrow \mathbb{R}$ is a continuous function that are piecewise linear on m subdomains

$$\Omega_i, \quad i = 1 : m.$$

Namely, on each Ω_i , f is a linear function:

$$f(x) = f_i(x) = a_i \cdot x + b_i, \quad x \in \Omega_i,$$

with some $a_i \in \mathbb{R}^d$ and $b_i \in \mathbb{R}$.

Lemma 5.1 *There are M number of subdomains,*

$$\tilde{\Omega}_k, \quad k = 1 : M,$$

such that

$$f_i - f_j \text{ does not change sign on each } \tilde{\Omega}_k, k = 1 : M.$$

Furthermore

$$m \leq M \leq m!$$

Proof Because m is finite, so there must exist M number of subdomains,

$$\tilde{\Omega}_k, \quad k = 1 : M$$

such that

$$f_i - f_j \text{ does not change sign on each } \tilde{\Omega}_k, k = 1 : M.$$

Then we proceed to estimate M . On the one hand, we have m pieces linear functions, so

$$M \geq m.$$

On the other hand, on each $\tilde{\Omega}$, we have the same rearrangement in ascending order of the values of the m linear functions. There are at most $m!$ possible rearrangements. Then we show that for any $\tilde{\Omega}_i$ and $\tilde{\Omega}_j$, they must be the same subdomain if they have the same rearrangement in ascending order. If not, there must exist a boundary formed by two linear functions l_p and l_q , and $\tilde{\Omega}_i$ and $\tilde{\Omega}_j$ must be on the different sides of the boundary. The order of the l_p and l_q must be opposite on $\tilde{\Omega}_i$ and $\tilde{\Omega}_j$, which leads to a contradiction. So

$$M \leq m!.$$

□

There is an important theorem named the lattice representation theorem for CPWL functions in \mathbb{R}^d , more details can be founded in [15].

Theorem 5.1 *For every continuous piecewise linear function $f : \mathbb{R}^n \rightarrow \mathbb{R}$ with finite pieces defined by the distinct local linear functions l_i , $1 \leq i \leq m$ and $\{\tilde{\Omega}_k\}_{k=1}^M$ be the unique-order subdomains. Then there exist finite non-empty subsets of $\{1, 2, \dots, m\}$, say s_k , $1 \leq k \leq M$, such that*

$$f(x) = \max_{1 \leq k \leq M} \{\min_{i \in s_k} l_i\}. \quad (5.1)$$

For the relationship between ReLU DNNs and CPWL functions, we have the next theorem with some estimation.

Theorem 5.2 *A continuous function $f : \mathbb{R}^d \rightarrow \mathbb{R}$ that are piecewise linear on m subdomains can be represented by a ReLU DNN. Furthermore,*

1. *the number of hidden layers is bounded by*

$$N_{\text{layer}} \leq \lceil \log_2(d+1) \rceil. \quad (5.2)$$

2. *the number of neurons*

$$N_{\text{neuron}} = \begin{cases} \mathcal{O}(d2^{mM+(d+1)(m-d-1)}) & \text{if } m \geq d+1, \\ \mathcal{O}(d2^{mM}) & \text{if } m < d+1. \end{cases} \quad (5.3)$$

here M , satisfying $m \leq M \leq m!$, is the number of subdomains as defined in Lemma 5.1.

In Theorem 5.2, a relatively shallow ReLU DNN is introduced. For any CPWL function in \mathbb{R}^d , we can use a ReLU DNN with at most $\log_2 \lceil (d+1) \rceil$ hidden layers to represent it. Moreover, the second part of Theorem 5.2 gives us size estimates on such neural networks.

The main result in Theorem 5.2 is not new, which can be found in [14]. In the next subsection, we will give an outline of the proof of Theorem 5.2 and in particular to derive the new estimate (5.3) on the number of neurons needed in the DNN representation. We will also discuss the application of this theorem to the simplicial finite element space in § 3.1.

5.2 On the proof of Theorem 5.2

In this section, we give an outline of the proof of Theorem 5.2. We will mainly follow the proof in [14] which is based on many relevant results in existing literature such as [14, 30], but add some detailed estimate of the number of neurons.

Lemma 5.2 *Let $f(\cdot)$, $g(\cdot)$ and $h(\cdot)$ be arbitrary functions from $\mathbb{R}^d \rightarrow \mathbb{R}$. If $\alpha \neq 1$, let $\bar{\alpha} = \frac{1}{1-\alpha}$. Then the following identity is valid for all $x \in \mathbb{R}^d$,*

$$\begin{aligned} \max\{f, g, \alpha g + h\} &= \max\{f, \max\{1, \alpha\} \max\{g - \bar{\alpha}h, 0\} + \bar{\alpha}h\} \\ &\quad + \max\{f, \min\{1, \alpha\} \min\{g - \bar{\alpha}h, 0\} + \bar{\alpha}h\} - \max\{f, \bar{\alpha}h\}. \end{aligned} \quad (5.4)$$

Moreover, we have:

$$\max\{f, g, \alpha g + h\} = \sigma_1 \max\{f, g, \bar{\alpha}h\} + \sigma_2 \max\{f, \alpha g + h, \bar{\alpha}h\} + \sigma_3 \max\{f, \bar{g}\}. \quad (5.5)$$

here $\sigma_k \in \{1, -1\}$ and \bar{g} is one of $g, \alpha g + h$ or $\bar{\alpha}h$.

Lemma 5.3 *For any interger L with $1 \leq n < L$, $c_0 \in \mathbb{R}$ and arbitrary linear function $l_1(x), \dots, l_L(x)$ of $x \in \mathbb{R}^d$, there exist finite groups of $L - 1$ linear functions, say $l(x, b_1(k)), \dots, l(x, b_{L-1}(k))$, $1 \leq k \leq K$, and corresponding $c_k \in \mathbb{R}$, $\sigma_k \in \{1, -1\}$ such that*

$$\max\{c_0, l_1, \dots, l_L\} = \sum_{k=1}^K \sigma_k \max\{c_k, l(x, b_1(k)), \dots, l(x, b_{L-1}(k))\}. \quad (5.6)$$

Lemma 5.4 *Let $f_1, \dots, f_m : \mathbb{R}^d \rightarrow \mathbb{R}$ be functions that can each be represented by $\mathbb{R}^d \rightarrow \mathbb{R}$ ReLU DNNs with depth $k_i + 1$ and size s_i . Then the function $f := \max\{f_1, \dots, f_m\}$ can be represented by a ReLU DNN of depth at most $\max\{k_1, \dots, k_m\} + \lceil \log m \rceil + 1$ and size at most $s_1 + \dots + s_m + 4(2m - 1)$.*

With all the lemmas above, now we can start to prove Theorem 5.2.

Proof For any continuous piecewise linear function f from \mathbb{R}^d to \mathbb{R} , we have the following lattice representation by Theorem 5.1:

$$f = \max_{1 \leq j \leq M} \min_{i \in s_j} l_i.$$

where M is the number of subdomains as defined in Lemma 5.1, and $s_j \subset \{1, \dots, m\}$, m is the number of distinct pieces of f .

Let $\Phi_j = \max_{1 \leq t \leq j} \{\min_{i \in s_t} l_i\}$, $1 \leq j \leq M$, then

$$f = \Phi_M = \max\{\Phi_{M-1}, \min_{i \in s_M} l_i\}. \quad (5.7)$$

Since

$$\begin{aligned} \max\{f, \min_{1 \leq i \leq m} l_i\} &= \sum_i \max\{f, l_i\} \\ &+ \cdots + (-1)^{m+1} \max\{f, l_1, \dots, l_m\}, \end{aligned}$$

we can write Equation (5.7) as:

$$f = \sum_{n=1}^{K_1} \sigma_n^{(1)} \max\{\Phi_{M-1}, \max_{i \in s_n^{(1)}} l_i\}, \quad (5.8)$$

with $K_1 \leq 2^m - 1$, $s_n^{(1)} \subset \{1, 2, \dots, m\}$ and $\sigma_n^{(1)} \in \{1, -1\}$.

For each $\max\{\Phi_{M-1}, \max_{i \in s_n^{(1)}} l_i\}$ in (5.8), we can continue this procedure for $M - 1$ times. Then we have:

$$f = \sum_{n=1}^{M'} \sigma_n \max_{i \in s'_n} l_i, \quad (5.9)$$

here $s'_n \subset \{1, 2, \dots, m\}$ and $M' \leq (2^m - 1)^M$.

Now that we write a piecewise linear function in form of (5.9), in order to get the $\lceil \log_2(d+1) \rceil$ -hidden-layer ReLU DNN, we need to do linear transformations to reduce the cardinality of s'_n from m to $n+1$. This can be done by Lemma 5.3.

Following the procedures in Lemma 5.3 by [30], when reducing one cardinality of s'_n , one $\max_{i \in s'_n} l_i$ will become at most $2^{d+1} - 1$ terms. If the cardinality is reduced from m to $d+1$, then we need to repeat the whole procedure $m - d - 1$ times. Hence for each $\max_{i \in s'_j} \{l_i\}$, in total we have at most $(2^{d+1} - 1)^{m-d-1}$ terms. Thus for

$$f = \sum_{j=1}^p s_j \max_{i \in S_j} l_i,$$

with $s_j \in \{-1, +1\}$ and $|S_j| \leq d+1$, we have $p \leq (2^m - 1)^M (2^{d+1} - 1)^{m-d-1}$.

For each $\max_{i \in S_j} l_i$ with $|S_j| \leq d+1$, Lemma 5.4 can be used to get a ReLU DNN with $\lceil \log_2(d+1) \rceil$ hidden layers. Again by Lemma 5.4, the size is at most

$2(d+1) + 4(2(d+1) - 1) = 10d + 6$. Adding these $\max_{i \in S_j} l_i$ together, we have the total size is at most $(10d+6)(2^m-1)^M(2^{d+1}-1)^{m-d-1}$, which is $\mathcal{O}(d2^{mM+(d+1)(m-d-1)})$.

Note that if $m \leq d+1$, we do not need to use Lemma 5.3, the size will be at most $\mathcal{O}(d2^{mM})$. \square

The estimation in Theorem 5.2 is a rough one, but still can provide some insights of this DNN representation. It can be seen that although the depth of this DNN is relatively shallow, the size of it might be extremely large, depending on the numbers of subdomains and distinct pieces.

5.3 Linear finite element functions as DNN with $\lceil \log_2(d+1) \rceil$ hidden layers

Given a locally convex finite element grid, now we have two different ways to represent a linear finite element function. In this part, we estimate the number of neurons if we write the function as a ReLU DNN with at most $\lceil \log_2(d+1) \rceil$ hidden layers. Then we can compare the sizes of two different approaches. Again we start with the basis functions.

Theorem 5.3 *Given x_i , denote the corresponding basis function as ϕ_i . If $G(i)$ is convex, then the ReLU DNN with at most $\lceil \log_2(d+1) \rceil$ hidden layers has size at most $\mathcal{O}(d2^{(d+1)k_h})$.*

Proof From Lemma 3.1, we know that

$$\phi_i(x) = \max \left\{ 0, \min_{k \in N(i)} g_k(x) \right\}.$$

For simplicity, let us further assume that

$$\phi_i = \max \left\{ 0, \min \{ g_{r_1}, \dots, g_{r_{|N(i)|}} \} \right\}.$$

The first step is to write it as the linear combination fo max functions

$$\begin{aligned}\phi_i &= \max \left\{ 0, \min \{g_{r_1}, \dots, g_{r_{|N(i)|}}\} \right\}, \\ &= \sum_{k \in N(i)} \max\{0, g_k\} + \dots + (-1)^{|N(i)|+1} \max\{0, g_{r_1}, \dots, g_{r_{|N(i)|}}\}.\end{aligned}$$

Our goal is to make every term on the right hand side only take maximum over at most $d + 1$ linear functions, here d is the dimension.

For any term with linear functions more than $d + 1$, we need to use linear transformation to reduce this number. When reducing by one, one term will become at most $2^{d+1} - 1$ terms. Thus $\max\{0, g_1, \dots, g_l\}$ will become at most $(2^{d+1} - 1)^{l-d}$ when $l \geq d$.

For any term with number of linear functions less or equal than $d + 1$, it remains unchanged. The number of this kind of terms is

$$C_{|N(i)|}^1 + C_{|N(i)|}^2 + \dots + C_{|N(i)|}^d.$$

Then in total the number of terms should be

$$N = \sum_{j=1}^d C_{|N(i)|}^j + \sum_{j=d+1}^{|N(i)|} C_{|N(i)|}^j (2^{d+1} - 1)^{j-d}.$$

Since any linear transformation $T : \mathbb{R}^d \rightarrow \mathbb{R}$ can be represented by a 2-layer ReLU DNN of size 2, for $\max_{i \in S} \{l_i\}$ with the number of $|S| \leq s$, it can be represented by a ReLU DNN of size at most $2s + 4(2s - 1) = 10s - 4$. So the total size is

$$\begin{aligned}S &= \sum_{j=1}^d C_{|N(i)|}^j (10j + 6) + (10d + 6) \sum_{j=d+1}^{|N(i)|} C_{|N(i)|}^j (2^{d+1} - 1)^{j-d}, \\ &= \mathcal{O}(d2^{(d+1)|N(i)|}), \\ &= \mathcal{O}(d2^{(d+1)k_h}).\end{aligned}$$

□

Corollary 5.1 *Given a locally convex finite element grid \mathcal{T}_h , any linear finite element function in \mathbb{R}^d with N degrees of freedom, can be written as a DNN function with at most $\lceil \log_2(d+1) \rceil$ hidden layers and with size at most $\mathcal{O}(d2^{(d+1)k_h}N)$.*

Proof According to Corollary 5.3, every basis function has a size independent of N , so the size of the DNN function with at most $(\lceil \log_2(d+1) \rceil)$ hidden layers is at most $\mathcal{O}(d2^{(d+1)k_h}N)$. \square

By comparing the above results with Theorem 3.1, we can see that although the DNN with $\lceil \log_2(d+1) \rceil$ hidden layers has shallower depth, the number of neurons is much larger than the one with $\lceil \log_2 k_h \rceil + 1$ hidden layers.

6 Low bit-width DNN models

In this section, we will show the rationality of low bit-width models with respect to approximation properties in some sense by investigating that a special type of ReLU DNN model can also recover all CPWL functions. In [17], an incremental network quantization strategy is proposed for transforming a general trained CNN into some low bit-width version in which their parameters are all zeros or powers of two. Mathematically speaking, low bit-width DNN model is defined as:

$$\text{DNN}_{k,l}^J := \{f = \Theta^J \circ \sigma \circ \Theta^{J-1} \dots \sigma \circ \Theta^0(x), \Theta_{i,j}^\ell \in \mathcal{Q}_{k,l}\}, \quad (6.1)$$

where σ is the activation function and

$$\mathcal{Q}_{k,l} := 2^k \times \{0, \pm 2^{1-2^{l-2}}, \pm 2^{2-2^{l-2}}, \dots, \pm 1\}. \quad (6.2)$$

In [17], they introduce a closed projected formula for finding the optimal approximation of vector $W^* \in \mathbb{R}^m$ in $\mathcal{Q}_{k,l}$.

$$\min_{s,W} \|W - W^*\|_F^2, \quad \text{subject to } W_i \in \mathcal{Q}_{k,l}. \quad (6.3)$$

Under this closed form, they propose a projected gradient descent method with respect to SGD to train a general R-FCN [31] model for object detection. They also

find that 6-bit (i.e $b = 6$) model works almost the same with classical model in the object detection tasks.

Then it comes the question: why can those kinds of models work? More precisely, for classification or detection problems, can this model separate those data exactly? By our results in previous sections, we find a special family of ReLU DNN which has at most one general layers and all other layers with low bit-width parameters. The results offer modification and theoretical explanation of the existing low bit-width DNNs proposed in the literature.

Here we try to explain why those low bit-width DNN model also work for classification problems to some extent. We have the following result:

Theorem 6.1 *Any continuous piecewise function can be represented by the next model:*

$$\widetilde{\text{DNN}}_{0,3}^J := \{f = \Theta^J \circ \text{ReLU} \circ \Theta^{J-1} \dots \text{ReLU} \circ \Theta^0(x), \Theta_{i,j}^\ell \in \mathcal{Q}_{0,3}, \forall \ell \geq 1, \Theta_{i,j}^0 \in \mathbb{R}\}, \quad (6.4)$$

with $\mathcal{Q}_{0,3}$ defined in (6.2) and $J \geq \lceil \log_2(d+1) \rceil$.

Proof Because of Theorem 5.2, we can rewrite any piecewise linear function as a ReLU DNN

$$f(x) = \Theta^{J_0} \circ \text{ReLU} \circ \Theta^{J_0-1} \circ \dots \circ \text{ReLU} \circ \Theta^0(x),$$

with $J_0 \leq \lceil \log_2(d+1) \rceil$. By (3.9), we know that

1. For each $\ell \geq 1$, we have

$$b^\ell = 0,$$

and $W^\ell = \{w_{ij}^\ell\}$ with $w_{ij}^\ell \in \{0, \pm 1, \pm 1/2\}$.

2. For $\ell = 0$, where we have a “fully connected layer”, the W^0, b^0 are determined by those linear functions.

Also note that $\widetilde{\text{DNN}}_{0,3}^{J_0} \subseteq \widetilde{\text{DNN}}_{0,3}^J$ if $J_0 \leq J$. This completes the proof.

□

Although we have the universal approximation property for DNN with a single hidden layer, in which model the last layer $\theta^1 \in \mathbb{R}^{n^1 \times 1}$ is still fully connected, this is a little bit different from the $\widetilde{\text{DNN}}_{0,3}^J$ models defined above.

7 Application to Numerical PDEs

In this section, we discuss the application of DNNs to the numerical solution of partial differential equations (PDEs). In most of our discussion, we consider the following model problem:

$$\begin{aligned} -\Delta u &= f, & x \in \Omega, \\ \frac{\partial u}{\partial \nu} &= 0, & x \in \partial\Omega, \end{aligned} \tag{7.1}$$

here $\Omega \subset \mathbb{R}^d$ is a bounded domain. For simplicity of exposition, we only consider Neuman boundary condition here. As it is done in the literature, special cares need to be taken for Dirichlet boundary value problems, but we will not get into those (standard) details.

The idea of using DNN for numerical PDEs can be traced back to [32] where a collocation method is used. Similar ideas have been explored by many different authors for different types of PDEs.

For the model problem (7.1), roughly speaking, the collocation method amounts to the following least square problem:

$$\min_{\Theta} \sum_{x_i \in \Omega} (-\Delta u_N(x_i, \Theta) - f(x_i))^2, \tag{7.2}$$

here $u_N(x, \Theta)$ is taken among the DNN function class in the form of (2.3) with a smooth activation function such as sigmoidal function and x_i are some collocation points.

Recently, [33] applied DNN for numerical PDE in the Galerkin setting which

amounts to the solution of the following energy minimization problem:

$$\min_{\Theta} \int_{\Omega} \left(\frac{1}{2} |\nabla u_N(x, \Theta)|^2 - f u_N(x, \Theta) \right) dx \quad (7.3)$$

Numerical experiments have demonstrated the potential of this approach. In the rest of this section, we will discuss a number of aspects of this approach from both theoretical and practical viewpoints. In particular, we will discuss its relationship with two popular finite element methods: adaptive finite element method and moving grid method.

7.1 The finite element method

The finite element approximation to (7.1) can be written as

$$\min_{v \in V_h} \int_{\Omega} \left(\frac{1}{2} |\nabla v(x)|^2 - f v(x) \right) dx, \quad (7.4)$$

where V_h is the finite element space as described in §3.1.

In the finite element setting, the optimization problem (7.4) is to find the coefficient (ν_i) as in (3.3) for a given finite element mesh \mathcal{T}_h . Some more sophisticated versions of the finite element method can be obtained by varying or optimizing \mathcal{T}_h so that more accurate finite element approximation can be obtained. Roughly speaking, there are two main approaches for optimizing \mathcal{T}_h : one is the adaptive finite element method and the other is the moving grid finite element method.

The adaptive finite element method is, roughly speaking, to vary \mathcal{T}_h by either coarsening or refining the grid. One main theoretical result is that a family of adapted grids \mathcal{T}_h with $\mathcal{O}(N)$ degrees of freedom can be obtained so that the corresponding adaptive finite element approximation u_N satisfies the following error estimate

$$|u - u_h|_{1,2,\Omega} \leq C N^{-\frac{1}{d}} |u|_{2, \frac{2d}{d+2}, \Omega}. \quad (7.5)$$

We refer to [29, 27] for relevant details and its generalizations.

One interesting observation is that the convergence rate $\mathcal{O}(N^{-\frac{1}{d}})$ in (7.5) deteriorate badly as d increases. Of course, error estimate in the form (7.5) depends on which Sobolev or Besov function classes that the solution u belongs to, namely what norms are used in the right hand side of (7.5). But regardless what function classes for the solution u , no asymptotic error estimate seems to be known in the literature that is better than $\mathcal{O}(N^{-\frac{1}{d}})$.

The moving grid method is, on the other hand, to optimize \mathcal{T}_h by varying the location of grid points while preserving topological structure of the grids (in particular the number of grid points remain unchanged). This approach proves to be effective in many applications, see [34, 35]. But there are very few theories on the error estimate like (7.5) in the moving grid method.

However, the H^1 approximation properties are still unclear even for DNN_1 . [36] proves a similar result for H^1 error estimate for $\text{DNN}_1^m(\Omega)$ with activation function $\sigma(x) = \cos(x)$. For general activation functions, or just for ReLU, it is an open problem.

7.2 DNN-Galerkin method

The finite element methods discussed above, including adaptive method and moving grid method, depend crucially on the underlying finite element grids. Numerical methods based on DNN, as we shall describe now, are a family of numerical methods that require no grids at all. This is reminiscent of the “mesh-less method” that have been much studied in recent years [38, 39, 37]. But the mesh-less method still requires the use of discretization points. The *DNN-Galerkin* method (as we shall call), namely the Galerkin version of the DNN-element method such as (7.3), goes one step further: it does not even need any discretization points! It is a totally point-free method!

Let us now give a brief discussion on the error estimate for the DNN-Galerkin method. We first recall a classic result by [6] for a DNN with one hidden layer of

$\mathcal{O}(N)$ DOFs (i.e. $\mathcal{O}(\frac{N}{d})$ neurons),

$$\inf_{v \in \text{DNN}_{1^d}^{\frac{N}{d}}(\Omega)} \|u - v\|_{0,2,\Omega} \lesssim \left(\frac{N}{d}\right)^{-\frac{1}{2}} C_u, \quad (7.6)$$

here we have

$$C_u := \int_{\mathbb{R}^d} |\omega|_{\Omega} |\hat{u}(\omega)| d\omega, \quad (7.7)$$

where \hat{u} is the Fourier transform of any extension of the original function defined in Ω to the entire space \mathbb{R}^d . Here we need to point that C_u might scale with dimension d . The dependence on d is improved by [40, 41]. Especially, [41] improve this constant to be polynomial in d .

7.3 An 1D example: a two point-boundary value problem

As a proof of concept, let us discuss a very simple one dimensional example. We focus on the following model problem:

$$\begin{aligned} -u''(x) &= f, & x \in (0, 1). \\ u(0) &= u(1) = 0. \end{aligned} \quad (7.8)$$

The exact solution $u \in H^1(0, 1)$ satisfies that

$$u = \arg \min_{v \in H_0^1(0,1)} E(v), \quad (7.9)$$

where

$$E(v) = \int_0^1 \left(\frac{1}{2} |v(x)'|^2 - f v(x) \right) dx.$$

Given a grid

$$\mathcal{T}_N : 0 = t_0 < t_1 < \dots < t_{N+1} = 1.$$

We define the space of ReLU DNNs with one hidden layer as follows:

$$U = \{u(x; t, \theta) | u(x; t, \theta) = \sum_{i=0}^N (\theta_{i+1} - \theta_i) \text{ReLU}(x - t_i)\},$$

where θ_i is the slope of piecewise linear function in $[t_{i-1}, t_i]$. In order to satisfy the condition $u(1; t, \theta) = 0$, we have the constraint

$$\theta_0 = 0, \quad \sum_{i=0}^{N+1} \theta_{i+1} (t_{i+1} - t_i) = 0.$$

We minimize the energy norm

$$(t, \theta) = \arg \min_{t, \theta} \int_0^1 \left(\frac{1}{2} |u'(x; t, \theta)|^2 - fu(x; t, \theta) \right) dx, \quad u(x; t, \theta) \in U.$$

where $t = (t_0, t_1, \dots, t_{N+1}), \theta = (\theta_0, \theta_1, \dots, \theta_{N+1})$. We do the alternate iteration as below,

$$\begin{aligned} \theta^{k+1} &= \arg \min_{\theta} \int_0^1 \left(\frac{1}{2} |u'(x; t^k, \theta)|^2 - fu(x; t^k, \theta) \right) dx, \\ t^{k+1} &= t^k - \eta \nabla_t \left(\int_0^1 \left(\frac{1}{2} |u'(x; t, \theta^{k+1})|^2 - fu(x; t, \theta^{k+1}) \right) dx \right), \end{aligned}$$

where η is the step-length. Once t is fixed, the minimization problem is a quadratic optimization, which is the traditional finite element method. So we solve the FEM solution $u(x; t^k, \theta^{k+1})$ on grid t and then compute the slope θ_i on each $[t_{i-1}, t_i]$.

We choose the exact solution as

$$u(x) = x(e^{-(x-\frac{1}{3})^2/K} - e^{-\frac{4}{9}/K}),$$

with $K = 0.01$. In this numerical experiment, the learning rate $\eta = 0.5$, the max iteration step is 200, and the degrees of freedom $N = 53$.

Algorithm 1 Simulation 1D PDE

Data: Grid t , Max iteration step M .

Result: Optimal solution $u(x; t^*, \theta^*)$.

Solve θ on the grid t ;

while $k \leq M$ **do**

$$g = \nabla_t \left(\int_0^1 \left(\frac{1}{2} |u'(x; t, \theta)|^2 - fu(x; t, \theta) \right) dx \right);$$

Find η by line search;

$$t \leftarrow t - \eta g;$$

Solve θ on the grid t ;

$$k \leftarrow k + 1;$$

end while

N	$ u_{uFEM} - u _1$	$ u_{AFEM} - u _1$	$ u_{DNN} - u _1$	$E(u_{uFEM})$	$E(u_{AFEM})$	$E(u_{DNN})$
23	0.2779	0.1375	0.1094	-0.7047	-0.7338	-0.7373
37	0.1717	0.0760	0.0663	-0.7285	-0.7404	-0.7411
53	0.1193	0.0511	0.0456	-0.7362	-0.7420	-0.7422

Table 1: The H^1 semi-norm error and energy

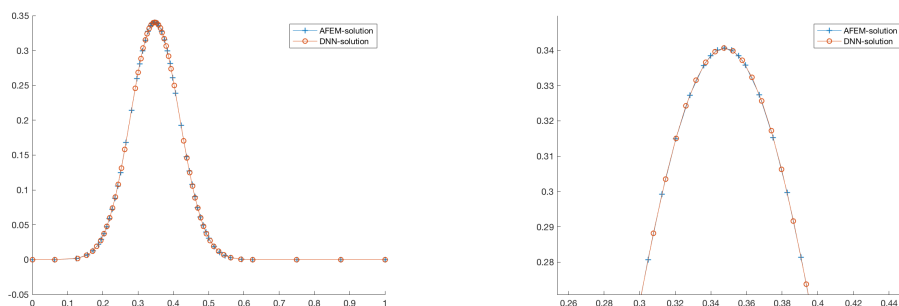


Figure 7.1: The grid of AFEM and DNN(the right figure is the top of left).

At the beginning of the simulation, we use the adaptive finite element method(AFEM) to get the adaptive grid from the uniform grid. Next we construct DNN solution with the same degrees of freedom. Then we minimize the energy and get the DNN solution. We compare the energy and H^1 semi-norm error of uniform grid solution(uFEM), AFEM solution and DNN solution. From Table 1, the energy and H^1 semi-norm of the DNN solution are smaller than u_{AFEM} and u_{uFEM} , which implies that the DNNs can find better solution than AFEM. Figure 7.1 shows the two different grid points on the same graph, we can easily see the grid points are moving.

8 Conclusion

By relating ReLU DNN models with linear finite element functions, we provide some theoretical insights on why and how deep neural networks work. It is shown that ReLU DNN models with sufficiently many layers (at least two) can reproduce all the linear finite element functions. This in some sense provides some theoretical explanation of the expressive power of deep learning models and also the necessity of using deep layers in deep learning applications.

Two different approaches are discussed in this paper on the representation of continuous piecewise linear functions by ReLU DNNs. The first approach, as proposed in [14] and described in §5, leads to a DNN representation with a relatively shallow network with $\lceil \log_2(d+1) \rceil$ hidden layers but a relatively larger number of neurons. The second approach, presented in this paper and described in §3, leads to a representation that has a relatively deeper network with $\lceil \log_2 k_h \rceil + 1$ hidden layers (see (3.4)). Further investigations are needed in the future to combine these two approaches to obtain a more balanced representation.

The DNN representation of linear finite element functions opens a door for theoretical explanation and possible improvement on the application of the quantized weights in a convolution neural networks (see [17]).

One theoretically interesting question addressed in this paper concerns the minimal number of layers that are needed in a DNN model to reproduce general continuous piecewise linear functions. Theorem 4.1 provides a partial answer to this

question, namely the minimal number of layers is at least 2. As a result, the number of layers $\lceil \log_2(d+1) \rceil$ as given in Theorem 5.2 is optimal for $1 \leq d \leq 3$. It is still an open question if this number is also optimal for $d \geq 4$.

This paper also briefly touches upon the application of DNN in numerical solution of partial differential equations, which is a topic that was investigated in the literature in 1990s and has attracted much attention recently. Our focus is on the comparison of Galerkin type of discretization methods provided by adaptive linear finite element methods and by deep neural networks. When the dimension d is large, asymptotic approximation properties are compared for these two different approaches in terms of the number of the dimension d and the number of the degrees of freedom. When d is small, we use the simplest case $d = 1$ to demonstrate that the deep neural network would lead to a more accurate Galerkin approximation to a differential equation solution than the adaptive finite element method would under the assumption that the degrees of freedom are the same in both cases but without comparing their computational costs. This preliminary study seems to indicate that deep neural network may provide a potentially viable approach to the numerical solution of partial differential equations for both high and low dimensions although the underlying computational cost is a serious issue that may or may not be properly addressed by further studies in the future.

A Lattice representation

In this section, we will discuss the lattice representation of CPWL functions in Theorem 5.1. To begin with, let us recall Lemma 5.1, where we have M subdomains $\{\tilde{\Omega}_k\}$ such that on each subdomain the arrangement of the m local functions are fixed. We denote this kind of domain partition as unique-order region partition.

Lemma A.1 *Let $p(t)$ be a continuous piecewise linear function and the unique-order region partition is*

$$0 = t_0 < t_1 < \dots < t_{r+1} = 1$$

assume the linear function on $[t_i, t_{i+1}]$ is $l_i(x) = k_i t + b_i$. If the parameters satisfy

$$b_0 > b_r, \quad k_0 + b_0 > k_r + b_r$$

which means

$$l_0(t) > l_r(t) \quad \text{on} \quad [t_0, t_1]$$

$$l_0(t) > l_r(t) \quad \text{on} \quad [t_r, t_{r+1}]$$

Then there exists $l_p(t) = k_p t + b_p$, such that

$$b_p \geq b_0, \quad k_p + b_p \leq k_r + b_r$$

That is to say,

$$l_0(t) \leq l_p(t) \quad \text{on} \quad [t_0, t_1]$$

$$l_p(t) \leq l_r(t) \quad \text{on} \quad [t_r, t_{r+1}]$$

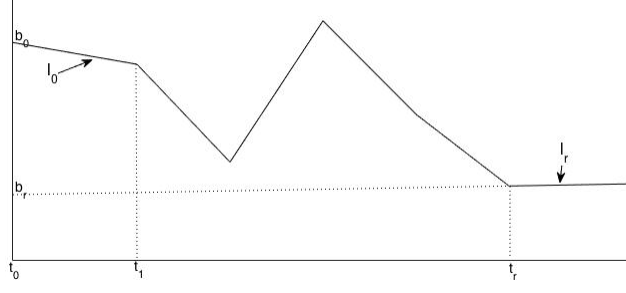
Proof

Let $k_p = \min_i \{k_i\}$, $\Delta t_i = t_{i+1} - t_i$.

Since here we only involve linear functions, so we can represent each point (t_i, y_i) by using k_i 's and Δt_i 's.

Then the point $(t_p, b_0 + \sum_{i=0}^{p-1} k_i \Delta t_i)$ is on $y = k_p t + b_p$, and we can write b_p as following:

$$b_p = b_0 + \sum_{i=0}^{p-1} k_i \Delta t_i - k_p t_p = b_0 + \sum_{i=0}^{p-1} (k_i - k_p) \Delta t_i$$



Since here k_p is the minimum, we have:

$$b_p = b_0 + \sum_{i=0}^{p-1} (k_i - k_p) \Delta t_i \geq b_0$$

And

$$k_p + b_p = k_p + b_0 + \sum_{i=0}^{p-1} (k_i - k_p) \Delta t_i$$

$$k_r + b_r = k_r + b_0 + \sum_{i=0}^{r-1} (k_i - k_p) \Delta t_i$$

$$(k_r + b_r) - (k_p + b_p) = k_r - k_p + \sum_{i=p}^{r-1} (k_i - k_p) \Delta t_i \geq 0$$

which means we find the desired pair of k and p .

Notice here $k_p \neq k_0$ and $k_p \neq k_r$ by the assumptions in the lemma.

□

The proof of Theorem 5.1 is as below.

Proof

In each $\tilde{\Omega}_k$, consider the functions lie completely above l_k , and define the convex polynomial

$$\Phi_k = \min_{i \in s_k} l_i$$

here $s_k = \{i : l_i \geq l_k \text{ on } \tilde{\Omega}_k\}$.

It's easy to see that in each $\tilde{\Omega}_k$, $\Phi_k = l_k = f$. Then define

$$\Phi = \max_k \Phi_k$$

and next we show that $\Phi_k(x) \leq f(x)$ for all x and every k :

For any fixed k , $\forall x \in \mathbb{R}^n$, if $x \in \tilde{\Omega}_k$, then $\Phi_k(x) = l_k(x) = f(x)$.

If $x \notin \tilde{\Omega}_k$, then we suppose $x \in \tilde{\Omega}_{k'}$, so $f(x) = l_{k'}(x)$. Notice that here we have unique-order region, thus in each $\tilde{\Omega}_i$, the order of l_k and $l_{k'}$ is fixed.

There're several situations:

(1) $l_{k'} \geq l_k$ in $\tilde{\Omega}_k$, then $\Phi_k(x) \leq l_{k'}(x) = f(x)$.

(2) $l_{k'} < l_k$ in $\tilde{\Omega}_k$, then we consider the domain $\tilde{\Omega}_{k'}$:

(2a) $l_{k'} \geq l_k$ in $\tilde{\Omega}_{k'}$. In this case we have:

$$\Phi_k(x) \leq l_k(x) \leq l_{k'}(x) = f(x)$$

(2b) $l_{k'} < l_k$ in $\tilde{\Omega}_{k'}$. We take $x \in \tilde{\Omega}_k^\circ, x' \in \tilde{\Omega}_{k'}^\circ$. Then we have a path $L(\theta)$, the coordinate of the path is defined as $(x + \theta(x' - x), f(x + \theta(x' - x)))$ with $\theta \in [0, 1]$ (see Figure A). It is just a piecewise linear function with the parameter θ . Notice that the domain partition is now unique-order. So if we want to compare the order of the linear function, we just compare one point value in that region.

Then by Lemma A.1, there must exist l_t with $t \neq k, k'$ and

$$l_t \leq l_{k'} \quad \text{on } \tilde{\Omega}_{k'}$$

$$l_t \geq l_k \quad \text{on } \tilde{\Omega}_k$$

Then we should have:

$$\Phi_k(x) \leq l_t(x) \leq l_{k'}(x) = f(x)$$

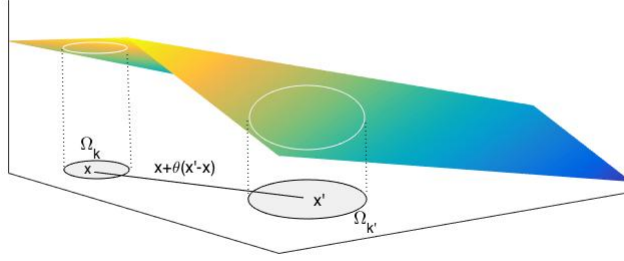


Figure A.1: Parameterization of the path.

Thus for every Φ_k , we have $\Phi_k(x) \leq f(x)$ for all x . So if we take the maximum over all these functions, we should have:

$$f(x) = \max_k \min_{i \in s_k} \{l_i\}$$

This is exactly the desired form. Here $|s_k| \leq m$, and the number of Φ_k depends on the domain partition we do.

□

The drawback of this representation is that the number of M may be too large, so we want to deal with other domain partitions, for example, partitions that produce a set of convex regions. The following theorem is an improvement of Theorem 5.1.

Theorem A.1 *Let $f : \mathbb{R}^d \rightarrow \mathbb{R}$ be a continuous piecewise linear function with finite pieces defined by the distinct local linear functions l_i , $1 \leq i \leq m$. Let $\{C_k\}$ be a set of S convex regions of f that determine a domain partition, so that the function f is described in each region C_k by the same linear function l_k . Then there exist finite non-empty subsets of $\{1, 2, \dots, m\}$, say s_k , $1 \leq k \leq S$, such that*

$$f(x) = \max_{1 \leq k \leq S} \{ \min_{i \in s_k} l_i \} \tag{A.1}$$

Proof In each C_k , define:

$$\Psi_k = \min_{i \in s_k} l_i$$

here $s_k = \{i : l_i \geq l_k \text{ on } C_k\}$. Then define:

$$\Psi = \max_{1 \leq k \leq S} \Psi_k$$

We should have $f = \Psi$ for all x .

If the arrangement inside a convex region C_k is the same, then the proof should be the same as Theorem 5.1. If not, the contribution of each region C_k can be considered as the union of the contributions of its unique-order subsets: $\Psi_k = \max_{1 \leq i \leq M_k} \Phi_i$, here Φ_i is defined as in Theorem 5.1. We can see that $\sum_{k=1}^S M_k$ is no less than M , the number of unique-order regions. By applying properties of lattices, we have:

$$\Psi = \max_{1 \leq k \leq S} \Psi_k = \max_{1 \leq i \leq M} \Phi_i$$

so according to Theorem 5.1, $\Psi = f$ for all x in the domain. □

B Proof of Lemmas

In this section, we will show the proofs of the lemmas used in previous sections.

B.1 Proof of Lemma 5.2

Proof We have the identity

$$\begin{aligned} \max\{f, g, \alpha g + h\} &= \max\{f, \max\{g, \alpha g + h\}\} \\ &= \max\{f, \max\{g - \bar{\alpha}h, \alpha g + h - \bar{\alpha}h\} + \bar{\alpha}h\} \\ &= \max\{f, \max\{g - \bar{\alpha}h, \alpha(g - \bar{\alpha}h)\} + \bar{\alpha}h\} \end{aligned} \tag{B.1}$$

When $\alpha > 1$, if $g - \bar{\alpha}h \geq 0$, then (B.1) becomes

$$\max\{f, \max\{1, \alpha\} \max\{g - \bar{\alpha}h, 0\} + \bar{\alpha}h\}$$

and the right hand side (RHS) of (5.4) becomes the same.

If $g - \bar{\alpha}h \leq 0$, then (B.1) becomes

$$\max\{f, \min\{1, \alpha\} \min\{g - \bar{\alpha}h, 0\} + \bar{\alpha}h\}$$

and the RHS of (5.4) is also this expression.

For $\alpha < 1$, similarly, the identity (5.4) always holds. Further, if consider the cases $\alpha > 1$, $0 < \alpha < 1$ and $\alpha < 0$ respectively, we have the following important identity:

$$\max\{f, g, \alpha g + h\} = \sigma_1 \max\{f, g, \bar{\alpha}h\} + \sigma_2 \max\{f, \alpha g + h, \bar{\alpha}h\} + \sigma_3 \max\{f, \bar{g}\} \quad (\text{B.2})$$

here $\sigma_k \in \{1, -1\}$ and \bar{g} is one of g , $\alpha g + h$ or $\bar{\alpha}h$. □

B.2 Proof of Lemma 5.3

Proof Let $l_i(x) = a_{i0} + \bar{a}_i^T x$ with $a_{i0} \in \mathbb{R}$ and $\bar{a}_i \in \mathbb{R}^n$ for $1 \leq i \leq L$. Assume there are at most \bar{n} linearly independent \bar{a}_i , $\bar{n} \leq n$. Without loss of generality, assume $\bar{a}_1, \dots, \bar{a}_{\bar{n}}$ are linearly independent. Then by basic linear algebra, we know that

$$l_L = \sum_{j=1}^{\bar{n}} \alpha_j l_j + \alpha_0.$$

Denote

$$\mu(x) = \max\{l_{\bar{n}+1}, \dots, l_{L-1}\}.$$

Then

$$\max\{c_0, l_1, \dots, l_L\} = \max\{c_0, l_1, \dots, l_{\bar{n}}, \mu(x), l_L\}. \quad (\text{B.3})$$

If $\alpha_j = 0$ for each $1 \leq j \leq \bar{n}$, then by taking $\max\{c_0, \alpha_0\}$, we already make the RHS of (B.3) as the RHS of (5.6). Otherwise, $\exists \alpha_j \neq 0$ for some $1 \leq j \leq \bar{n}$, we can assume that $\alpha_\eta \neq 0, \alpha_{\eta+1} = \dots = \alpha_{\bar{n}}$, so

$$l_L = \sum_{j=1}^{\eta} \alpha_j l_j + \alpha_0, \quad \eta \leq \bar{n}.$$

If $\alpha_i = 1$ for each $1 \leq i \leq \eta$, we can do the following linear transformation $(l'_1, \dots, l'_\eta)^T = A(l_1, \dots, l_\eta)^T$, where

$$\begin{aligned} l'_i &= l_i, & \text{for } i \neq \eta, \\ l'_i &= \sum_{j=1}^{\eta} l_j + \alpha_0, & \text{for } i = \eta. \end{aligned}$$

Then (B.3) equals

$$\max\{c_0, l'_1, \dots, l'_\eta, \mu(x), -\alpha_0 - l'_1 - \dots - l'_{\eta-1} + l'_\eta\}.$$

in this case, the coefficients of $l'_1, \dots, l'_{\eta-1}$ are not 1.

So we can assume there is at least one $\alpha_i \neq 1$ for $1 \leq i \leq \eta$, say $\alpha_\eta \neq 1$. Let

$$\begin{aligned} f &= \max\{c_0, \mu(x), l_1, \dots, l_{\eta-1}, l_{\eta+1}, \dots, l_\eta\}, \\ g &= l_\eta, \\ h &= \sum_{j=1}^{\eta-1} \alpha_j l_j + \alpha_0. \end{aligned}$$

by (5.5) we have:

$$\max\{c_0, l_1, \dots, l_\eta, \mu(x), l_L\} = \max\{f, g, \alpha_\eta g + h\} \quad (\text{B.4})$$

$$= \sigma_1 \max\left\{f, g, \frac{\sum_{j=1}^{\eta-1} \alpha_j l_j + \alpha_0}{1 - \alpha_\eta}\right\} \quad (\text{B.5})$$

$$+ \sigma_2 \max\left\{f, \alpha_\eta g + h, \frac{\sum_{j=1}^{\eta-1} \alpha_j l_j + \alpha_0}{1 - \alpha_\eta}\right\} \quad (\text{B.6})$$

$$+ \sigma_3 \max\{f, \bar{g}\}. \quad (\text{B.7})$$

(B.7) is already the desired form, because now we only take maximum over $L - 1$ linear functions and one constant.

As for the (B.5), notice that now we have eliminated l_η in the third expression. So continue this procedure, at last we will only have constant in the last expression, by taking maximum of this constant and c_0 , we can reduce one term in the max expression.

For (B.6), consider the linear transformation $(l''_1, \dots, l''_{\bar{n}})^T = B(l_1, \dots, l_{\bar{n}})^T$:

$$l''_i = l_i, \quad \text{for } i \neq \eta,$$

$$l''_i = \sum_{j=1}^{\eta} \alpha_j l_j + \alpha_0, \quad \text{for } i = \eta.$$

So (B.6) becomes

$$\max\{c_0, \mu, l''_1, \dots, l''_{\bar{n}}, \sum_{j=1}^{\eta-1} \alpha_j l''_j + \alpha_0\}.$$

Then it is the same as (B.5). Follow the same steps as for (B.5), we can achieve the desired result. \square

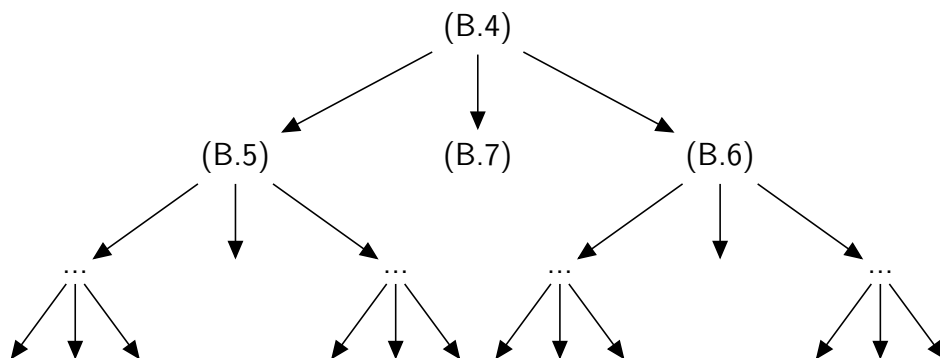


Figure B.1: The process of reducing one term.

Remark 2 Whenever we eliminate one l_i in the expression of l_L , we will gain 3 terms, which is (B.5-B.7). Among these three terms, (B.7) is in desired form, and we need to continue to use (5.5) for (B.5) and (B.6) until we only have constant.

Note that in the proof, $\eta \leq n$. By this procedure, we will gain at most $2^{n+1} - 1$ terms (see Figure B.2).

B.3 Proof of Lemma 5.4

Proof We prove the lemma by induction. When $m = 1$, the case is trivial. When $m \geq 2$, consider $g_1 := \max\{f_1, \dots, f_{\lfloor \frac{m}{2} \rfloor}\}$ and $g_2 := \max\{f_{\lceil \frac{m}{2} \rceil}, \dots, f_m\}$. By induction hypothesis, g_1 and g_2 can be represented by ReLU DNNs of depths at most $\max\{k_1, \dots, k_{\lfloor \frac{m}{2} \rfloor}\} + \lceil \log(\lfloor \frac{m}{2} \rfloor) \rceil + 1$ and $\max\{k_{\lceil \frac{m}{2} \rceil}, \dots, k_m\} + \lceil \log(\lceil \frac{m}{2} \rceil) \rceil + 1$ respectively, and sizes at most $s_1 + \dots + s_{\lfloor \frac{m}{2} \rfloor} + 4(2\lfloor \frac{m}{2} \rfloor - 1)$ and $s_{\lceil \frac{m}{2} \rceil} + 4(2\lceil \frac{m}{2} \rceil - 1)$ respectively. Then consider the function $F : \mathbb{R}^n \rightarrow \mathbb{R}^2$ defined as $F(x) = (g_1(x), g_2(x))$, this can be represented by a ReLU DNN with depth at most $\max\{k_1, \dots, k_m\} + \lceil \log(\lceil \frac{m}{2} \rceil) \rceil + 1$ and size at most $s_1 + \dots + s_m + 4(2m - 2)$.

Since $\max\{x, y\}$ can be represented by a 2-layer ReLU DNN with size 4, we know that f can be represented by a ReLU DNN of depth at most $\max\{k_1, \dots, k_m\} + \lceil \log(m) \rceil + 1$ and size at most $s_1 + \dots + s_m + 4(2m - 1)$. \square

References

- [1] Y. LeCun, Y. Bengio and G. Hinton, Deep learning, *nature*, **521**(2015), 436.
- [2] N. Cohen, O. Sharir and A. Shashua, On the expressive power of deep learning: A tensor analysis, in *Conference on Learning Theory*, 2016, 698-728.
- [3] K. Hornik, M. Stinchcombe and H. White, Multilayer feedforward networks are universal approximators, *Neural networks*, **2**(1989), 359-366.
- [4] G. Cybenko, Approximation by superpositions of a sigmoidal function, *Mathematics of control, signals and systems*, **2**(1989), 303-314.
- [5] L.K. Jones, A simple lemma on greedy approximation in Hilbert space and convergence rates for projection pursuit regression and neural network training, *The annals of Statistics*, **20**(1992), 608-613.

- [6] A.R. Barron, Universal approximation bounds for superpositions of a sigmoidal function, *IEEE Transactions on Information theory*, **39**(1993), 930-945.
- [7] S.W. Ellacott, Aspects of the numerical analysis of neural networks, *Acta numerica*, **3**(1994), 145-202.
- [8] A. Pinkus, Approximation theory of the MLP model in neural networks, *Acta numerica*, **8**(1999), 143-195.
- [9] M. Leshno, V.Y. Lin, A. Pinkus and S. Schocken, Multilayer feedforward networks with a nonpolynomial activation function can approximate any function, *Neural networks*, **6**(1993), 861-867.
- [10] V. Nair, and G. Hinton, Rectified linear units improve restricted boltzmann machines, in *Proceedings of the 27th international conference on machine learning (ICML-10)*, 2010, 807-814.
- [11] U. Shaham, A. Cloninger and R.R. Coifman, Provable approximation properties for deep neural networks, *Applied and Computational Harmonic Analysis*, 2016.
- [12] J.M. Klusowski and A.R. Barron, Approximation by Combinations of ReLU and Squared ReLU Ridge Functions with l^1 and l^0 Controls, 2018.
- [13] D.X. Zhou, Universality of Deep Convolutional Neural Networks, *arXiv preprint arXiv:1805.10769*, 2018.
- [14] R. Arora, A. Basu, P. Mianjy and A. Mukherjee, Understanding deep neural networks with rectified linear units, *arXiv preprint arXiv:1611.01491*, 2016.
- [15] J.M. Tarela and M.V. Martinez, Region configurations for realizability of lattice piecewise-linear models, *Mathematical and Computer Modelling*, **30**(1999), 17-27.
- [16] P.G. Ciarlet, The finite element method for elliptic problems, *Classics in applied mathematics*, **40**(2002), 1-511.

- [17] P. Yin, S. Zhang, J. Lyu, S. Osher, Y. Qi and J. Xin, BinaryRelax: A Relaxation Approach For Training Deep Neural Networks With Quantized Weights, *arXiv preprint arXiv:1801.06313*, 2018.
- [18] Y. LeCun, L. Bottou, Y. Bengio and P. Haffner, Gradient-based learning applied to document recognition, *Proceedings of the IEEE*, **86**(1998), 2278-2324.
- [19] A. Krizhevsky and G. Hinton, Learning multiple layers of features from tiny images, Technical report, University of Toronto, 2009.
- [20] F. Li, B. Zhang and B. Lin, Ternary weight networks, *arXiv preprint arXiv:1605.04711*, 2016.
- [21] D. Gobovic and M.E. Zaghloul, Analog cellular neural network with application to partial differential equations with variable mesh-size, in *Circuits and Systems, 1994. ISCAS'94., 1994 IEEE International Symposium on*, IEEE, 1994, 359-362.
- [22] A.J. Meade Jr and A.A. Fernandez, The numerical solution of linear ordinary differential equations by feedforward neural networks, *Mathematical and Computer Modelling*, **19**(1994), 1-25.
- [23] A.J. Meade Jr and A.A. Fernandez, Solution of nonlinear ordinary differential equations by feedforward neural networks, *Mathematical and Computer Modelling*, **20**(1994), 19-44.
- [24] W. E, J. Han and A. Jentzen, Deep learning-based numerical methods for high-dimensional parabolic partial differential equations and backward stochastic differential equations, *Communications in Mathematics and Statistics*, **5**(2017), 349-380.
- [25] J. Han, A. Jentzen, and W. E, Overcoming the curse of dimensionality: Solving high-dimensional partial differential equations using deep learning, *arXiv preprint arXiv:1707.02568*, 2017.

- [26] Y. Khoo, J. Lu and L. Ying, Solving parametric PDE problems with artificial neural networks, *arXiv preprint arXiv:1707.03351*, 2017.
- [27] R.A. DeVore, Nonlinear approximation, *Acta numerica*, **7**(1998), 51-150.
- [28] S. Brenner and R. Scott, *The mathematical theory of finite element methods(Vol. 15)*, Springer Science & Business Media, 2007.
- [29] R.H. Nochetto and A. Veeger, Primer of adaptive finite element methods, in *Multiscale and adaptivity: modeling, numerics and applications*, Springer, Berlin, Heidelberg, 2011, 125-225.
- [30] S. Wang and X. Sun, Generalization of hinging hyperplanes, *IEEE Transactions on Information Theory*, **51**(2005), 4425-4431.
- [31] J. Dai, Y. Li, K. He and J. Sun, R-fcn: Object detection via region-based fully convolutional networks, in *Advances in neural information processing systems*, Curran Associates, Inc., 2016, 379-387.
- [32] I.E. Lagaris, A. Likas and D.I. Fotiadis, Artificial neural networks for solving ordinary and partial differential equations, *IEEE Transactions on Neural Networks*, **9**(1998), 987-1000.
- [33] W. E and B. Yu, The Deep Ritz Method: A Deep Learning-Based Numerical Algorithm for Solving Variational Problems, *Communications in Mathematics and Statistics*, **6**(2018), 1-12.
- [34] R. Li, T. Tang and P. Zhang, Moving mesh methods in multiple dimensions based on harmonic maps, *Journal of Computational Physics*, **170**(2001), 562-588.
- [35] R. Li, T. Tang and P. Zhang, A moving mesh finite element algorithm for singular problems in two and three space dimensions, *Journal of Computational Physics*, **177**(2002), 365-393.

- [36] J. Xu, Deep Neural Networks and Multigrid Methods(Lecture Notes), Penn State University, 2017.
- [37] S.R. Idelsohn, E. Onate, N. Calvo and F.D. Pin, The meshless finite element method, *International Journal for Numerical Methods in Engineering*, **58**(2003), 893-912.
- [38] G.R. Liu, *Mesh free methods: moving beyond the finite element method*,CRC press, 2002.
- [39] G. Yagawa and T. Yamada, Free mesh method: a new meshless finite element method, *Computational Mechanics*, **18**(1996), 383-386.
- [40] V. Kurková and M. Sanguineti, Comparison of worst case errors in linear and neural network approximation, *IEEE Transactions on Information Theory*, **48**(2002), 264-275.
- [41] H.N. Mhaskar, On the tractability of multivariate integration and approximation by neural networks, *Journal of Complexity*, **20**(2004), 561-590.